Available online at www.sciencedirect.com

ScienceDirect

materialstoday: PROCEEDINGS

Materials Today: Proceedings 3S (2016) S227 – S232

Proceedings of the International Conference on Diamond and Carbon Materials

New graphene/ionic liquid nanolubricants

Noelia Saurín*, José Sanes, María-Dolores Bermúdez

Grupo de Ciencia de Materiales e Ingeniería Metalúrgica. Universidad Politécnica de Cartagena. 30202-Cartagena (Spain)

Abstract

In this work, we have prepared new graphene/ionic liquid dispersions by adding a 0.1wt.% proportion of 1-2 layers graphene (G1) or 1-10 layers graphene (G2) to the ionic liquid 1-octyl-3-methylimidazolium tetrafluoroborate (IL). The new dispersions (IL+G1) and (IL+G2) have been used as external lubricants in polymer-steel and ceramic-steel contacts. For AISI 316L stainless steel/epoxy resin, the order of friction reduction is (IL+G2)>IL>(IL+G1). The wear reducing order is the same, as abrasive wear takes place for (IL+G1), while G2 prevents any degree of surface damage on both materials, even the very mild wear observed for neat IL. The poor performance of G1 is related to the formation of abrasive graphene-IL aggregates. The (IL+G2) dispersion also shows superior friction reducing and anti-wear behavior under more severe contact conditions, for AISI316L against sapphire.

© 2016 The Authors. Published by Elsevier Ltd. This is an open access article under the CC BY-NC-ND license (http://creativecommons.org/licenses/by-nc-nd/3.0/).
Selection and Peer-review under responsibility of the chairs of the International Conference on Diamond and Carbon Materials 2014.

Keywords: Epoxy resin; stainless steel; sapphire; ionic liquid; graphene; nanolubricants; friction; wear.

1. Introduction

Graphene, constituted by one-atom thick layers of sp^2 carbon [1], has risen and extraordinary scientific and technical interest [2]. At the present moment, there exist diverse preparation methods [3] and very different commercial qualities of graphene. The tribological and surface science applications of graphene are some of the most front edge lines of research at the present moment [4, 5]. There exist very few precedents of the use of graphene in friction and wear reduction [4-9]. A 26% friction reduction and a 9% wear reduction were reported by Choudhary et al. [9], for steel by lubrication with hexadecane containing chemically modified graphene, by intercalation between the sliding surfaces. However, a diversity of friction behaviours have been found between different bi-layer graphenes [10]. The use of hybrid graphene nanocomposites has increased due to its effect in the improvement of polymer properties.

* *E-mail address:noelia.saurin@upct.es*

2214-7853 © 2016 The Authors. Published by Elsevier Ltd. This is an open access article under the CC BY-NC-ND license (http://creativecommons.org/licenses/by-nc-nd/3.0/).
Selection and Peer-review under responsibility of the chairs of the International Conference on Diamond and Carbon Materials 2014.
doi:10.1016/j.matpr.2016.02.038

The wear rate of polytetrafluoroethylene (PTFE) is reduced in four orders of magnitude by addition of a 10% of graphene sheets of 3-4 layers as nano-reinforcements [11, 12]. These authors have proposed that the graphene sheets could reduce wear by inhibiting crack propagation. Recent studies have shown that room temperature ionic liquids (ILs) can lower wear and friction in steel-polymer contacts [13, 14] among many other high performance tribological applications [15-19]. The effect of the use of ionic liquid (IL) as an internal lubricant in epoxy-IL composites in pin-on-disk friction tests has been previously studied [13]. Chemical modification of graphene has been described by covalent and non-covalent interactions [20]. Covalent modifications could modify the graphene conjugation system and its properties. Non-covalent modification by π–π stacking and van der Waals interactions, are believed to maintain the structure and properties of graphene. The combination of graphene and ionic liquids is being explored as novel lubricants for friction and wear reduction [21, 22]. We have recently described [23] the good tribological performance of epoxy matrix nanocomposites modified by dispersion of graphene modified by ionic liquid. In the present study, graphene-IL dispersions with non-covalent interactions between two different commercial graphene qualities and IL have been produced under mild conditions and used as external lubricants, and compared with the neat IL. The IL selected for the present study has previously demonstrated an excellent lubricanting performance [15] combines a high thermal stability with a high molecular polarity, which allows the formation of adsorbed layers on metal surfaces, and the presence of a long alkyl side chain which could improve the compatibility of nanophases with the polymer network. These properties have been tested, in the present work, in epoxy resin(ER)-steel contacts. The high load carrying ability of graphene and the high thermal stability of the IL lubricant anticipate a good tribological performance of graphene-IL dispersions also under the more severe conditions, thus we also present the results obtained for steel-ceramic lubrication.

2. Experimental

The IL 1-octyl-3-methylimidazolium tetrafluoroborate (purity >99%) from Iolitec, GmbH (Germany) and two commercially available graphene qualities were used, G1 (1-2 layers graphene from Avanzare Nanotechnology Spain) and G2 (1-10 layers graphene from Iolitec, Germany). To obtain the dispersions (IL+G1) and (IL+G2), G1 or G2 were added to the IL in a 0.1wt.% proportion, the mixtures were mechanically stirred in an agate mortar for five minutes and then at 1600 rpm for 30 seconds [23], finally the mixture was subjected under sonication for 30 min, 100%A and 30ºC. Epoxy resin disks were processed as previously described [23]. Transmission electron microscopy (TEM) and scanning electron microscopy (SEM), Raman spectroscopy and X-ray photoelectron spectroscopy (XPS) analysis techniques have been previously described [23]. For TEM, Raman and XPS, excess IL was removed from IL+G2 by repeatedly washing with acetonitrile and drying. Pin-on-disk tests were carried out with an ISC 200-PC pin-on-disk tribometer. For the polymer-metal contact, ER disks (diameter 40 mm; thickness 4 mm) against AISI 316L stainless steel balls (hardness 210 HV) with a 0.8 mm sphere radius were used under a normal applied load was 4.9 N (mean contact pressure 0.7 GPa), with a sliding velocity of 0.10 ms^{-1} and a sliding distance 500 m, for a sliding radius of 9 mm. For the ceramic-metal contact, sapphire (Al_2O_3, 99.9%) balls (Goodfellow Cambridge Ltd. UK) (Al_2O_3; 99.9 %; HV 2,750; Young's modulus 445 GPa; Poisson's ratio 0.24) of 0.75 mm sphere radius were tested against AISI 316L stainless steel disks (HV 200; Young modulus 197 GPa; Poisson's ratio 0.27; surface roughness R_a 0.05 μm) of 25 mm diameter and 5 mm thickness, under a normal applied load of 0.98 N (mean contact pressure 1.3 GPa), with a sliding velocity of 0.10 ms^{-1} and a sliding distance 500 m. Optical micrographs were obtained with a Leica DMRX microscope. Wear rates were determined by means of a Talysurf CLI profilometer. At least three tests were performed under the same experimental conditions for each material, at room temperature with a relative humidity of 40±5%.

3. Results and discussion

3.1. Characterization of IL+G2.

TEM microscopy and Raman spectroscopy studies of G1 and IL+G1 have been previously described [23]. Figure 1 shows TEM micrographs of as-received G2 (figure 1a) and IL+G2 (figure 1b), after removing the excess IL. Energy dispersive X-ray (EDX) analyses show the presence of up to a 12 wt.% of fluorine from the tetrafluoroborate anion in G2 after being treated with IL. Fig. 1c compares the Raman spectra of G2 as received, and after treatment with IL and removal of IL excess. No significant effect is observed due to the IL in the characteristic D (1361.2 cm^{-}

[1]), G (1596.6 cm^{-1}) and 2D (2951.6 cm^{-1}) bands. The I_D/I_G (0.79) and I_{2D}/I_G (0.31) intensity ratios are also similar in both cases, showing that the IL produces no significant effect on the proportion of defects present in G2 [3]. A similar result was obtained in the case of G1 and IL+G1 [23]. These results are in agreement with a non-covalent surface modification of graphene by IL, which has been also confirmed by XPS surface analysis. Fig. 2 shows the binding energies of the dry graphene after removal of excess IL form IL+G2. F1s (686.1 eV), N1s (402.0 eV) and B1s (194.2 eV) peaks are similar to those found for neat IL [23] and show the non-covalent surface modification of G2 by IL. The C1s peak at 285.0 eV is assignable to the aliphatic carbon (and to carbon impurities) atoms present in the alkyl substituents of the imidazolium ring. Two peaks assignable to sp^2 carbon atoms are observed at 286.6 and 287.6 eV, which could be assigned to the imidazolium ring and to graphene, respectively. The atomic proportions are in agreement with the presence of both the tetrafluoroborate anion and the imidazolium cation on G2 surface.

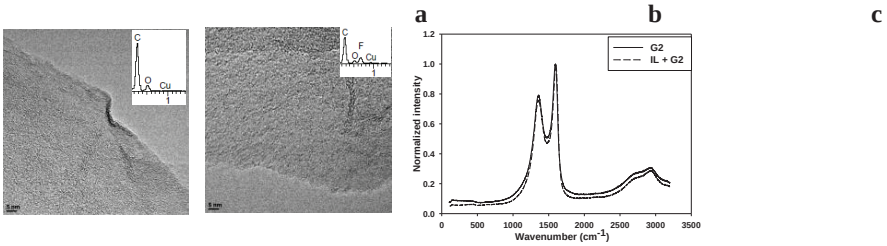

Fig. 1. TEM micrographs and EDX spectra: a) as-received G2; b) G2 after treatment with IL; c) Raman spectrum of as-received G2 and G2 after treatment with IL

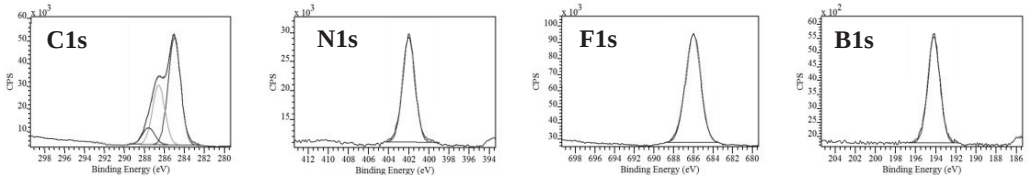

Fig. 2. XPS spectra of G2 after treatment with IL.

2.1. Tribological tests.

Figure 3a shows that the order of coefficient of friction (COF) reduction ability is (IL+G2)>IL>(IL+G1). Neat IL is a remarkably good lubricant for the ER/AISI316L system. This is in agreement with previous results for this IL as lubricant [17], which shows that for imidazolium ILs, a longer alkyl chain substitutent provides a lower friction coefficient due to a better ability to separate the sliding surfaces.

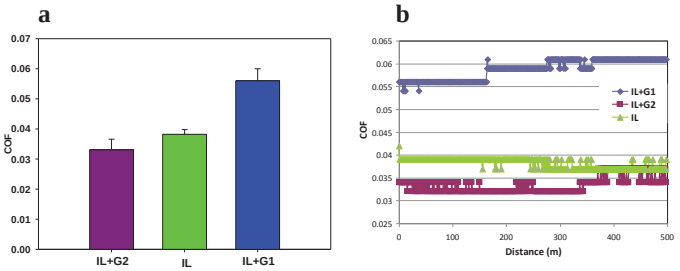

Fig. 3. ER/AISI 316L: a) Mean friction coefficients; b) Friction coefficient vs sliding distance.

The addition of G2 improves the load carrying ability of the lubricant reducing friction in a 13% with respect to IL. In contrast, the addition of G1 increases friction with respect to neat IL. When the friction coefficient-sliding distance records are observed (Fig. 3b) it can be seen that the presence of G2 reduces friction up to 400 m sliding distance. From that point to the end of the test, friction values are very similar for IL and for IL+G2. In contrast, the addition of G1 to IL has the opposite effect (Fig. 3a and 3b), increasing the friction coefficient of the ER/steel pair. This could be attributed to the presence of multilayered graphitic structures in G1, as previously described [23]. These structures would hinder the surface modification of graphene by IL molecules. Fig. 4 shows the steel ball surface (Fig. 4a) and the ER surface (Fig. 4b) after lubrication with IL. Abrasion marks are present on the steel

surface, while the ER wear rate is very mild (10^{-9} $mm^3N^{-1}m^{-1}$). Addition of G1, increases the abrasion of the steel ball (Fig. 5a), probably as a consequence of the G1 particles trapped on the sliding path (Fig. 5b).

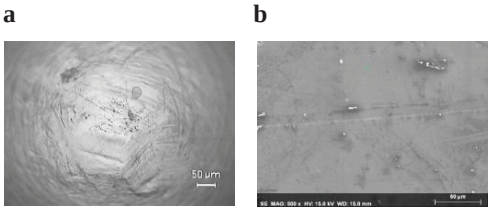

Fig. 4. SEM micrographs after lubrication with IL: a) AISI316L steel ball; b) Wear track on epoxy resin surface.

Fig. 5c shows the presence of fluorine due to the IL+G1 accumulated at the surface asperities on the ER surface, although the wear rate is negligible as can be observed in the surface topography (Fig. 5d).

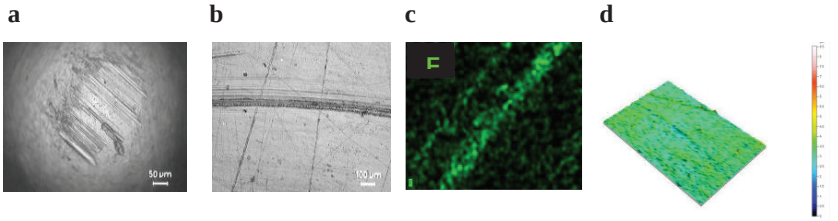

Fig. 5. Lubricantion with IL+G1: a) AISI316L stainless steel ball; b) Optical micrograph of epoxy resin; c) EDX fluorine element map of the wear path on epoxy resin; d) Surface topography of epoxy resin.

Fig. 6a-c shows that the IL+G2 dispersion presents excellent wear protection ability, preventing wear both of the steel ball and the ER disk.

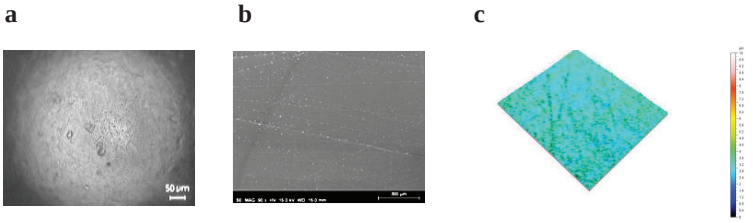

Fig. 6. a) Optical micrograph of AISI316L ball; b) SEM micrograph of epoxy resin; c) Surface topography of epoxy.

The excellent tribological behavior of IL+G2 in reducing friction and wear of ER/AISI316L was the reason for the selection of this dispersion as lubricant under more severe contact conditions in ceramic-metal contacts, AISI 316L/sapphire. Fig. 7a and b show that the addition of a 0.1wt.% G2 to IL reduces the mean friction coefficient value in a 16%. Similarly to the behavior observed in the ER/steel case (Fig. 3b), the maximum friction reduction due to G2 takes place in the initial running-in period, particularly during the first 100 m. This could be explained by the effective surface separation from the start of the sliding due to the interposition of the G2 particles, while neat IL needs an initial distance to form stable adsorbed layers of IL molecules.

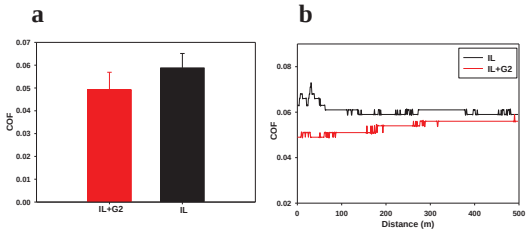

Fig. 7. Sapphire/AISI316L: a) Mean friction coefficients; b) Friction coefficient vs sliding distance.

The higher effectiveness of the IL+G2 dispersion can be observed in Fig. 8a-d. As expected, the sapphire ball shows no wear both for IL (Fig. 8a) and for IL+G2 (Fig.8b). Under lubrication with IL, the steel surface shows a wear track with plastic deformation and abrasion marks (Fig. 8c), while in the presence of IL+G2, the surface damage is milder (Fig. 8d). Wear rates of AISI316L calculated from wear track width according to ASTM G99 standard are of the same order of magnitude (10^{-7} $mm^3N^{-1}m^{-1}$) for both lubricants, with a 19% reduction for IL+G2 with respect to IL. Wear mechanisms can be determined from surface topography and profilometry studies (Figs. 9 and 10).

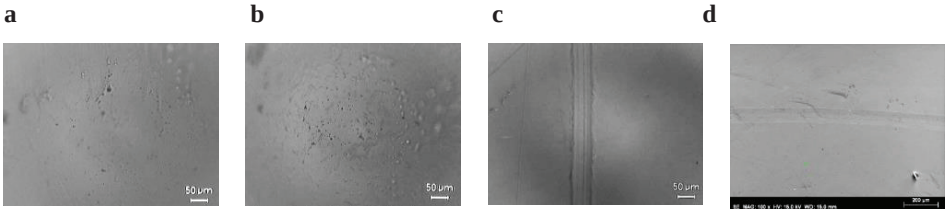

Fig. 8. Optical micrographs of sapphire balls: a) After lubrication with IL; b) After lubrication with IL+G2. AISI316L disk: c) After lubrication with IL; d) After lubrication with IL+G2.

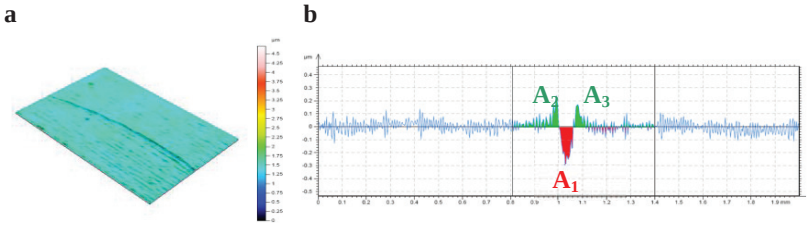

Fig. 9 a) Surface topography and b) cross section of wear track on AISI316L after lubrication with IL.

Surface topography shows abrasion marks under IL lubrication (Fig. 9a) which are almost negligible in the case of IL+G2 (Fig. 10a). Cross section areas (Figs. 9b and 10b) of material removed (in red) and plastically deformed material accumulated at the edges of the wear tracks (in green), confirm SEM microscopy and surface topography observations. The area of material removed (in red) from the stainless steel surface by the sapphire ball after lubrication with IL (Fig. 9b) is 14.51 μm^2, and the area of plastically deformed material accumulated on both edges (in green) is 16.22 μm^2. When IL is modified by the addition of G2 (Fig. 10b), the red area is reduced to 10.06 μm^2, while the maximum height of the material on the wear path edges (in green) is of the same order as the initial surface roughness, so there is no new material accumulated on the wear track edges.

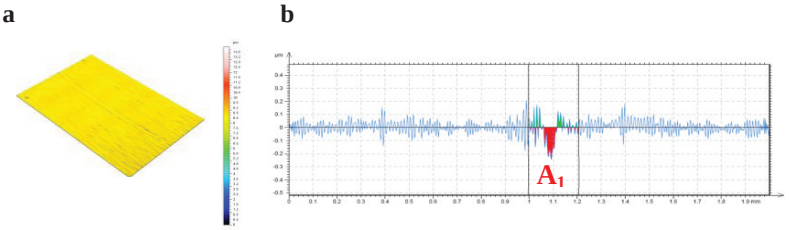

Fig. 10. a) Surface topography and b) cross section of wear track after lubrication with IL+G2.

The total surface damage can be quantified by the total area of plastically deformed material below and above the material surface, ie. $[A_1+(A_2+A_3)]$. In this way, a final surface damage reduction of a 67% is obtained for (IL+G2) with respect to IL, due to the less severe abrasion mechanism.

4. Conclusions

The addition of 1-2 layer graphene increases friction in epoxy resin-stainless steel contacts, with respect to the neat ionic liquid lubricant, due to the formation of graphene agglomerates at the interface which are retained on the epoxy resin surface and produce severe abrasion of the steel counterpart. The addition of the same proportion of dispersed 1-10 layers graphene particles reduces the friction coefficient and wear rate, both in epoxy resin-stainless steel and in stainless steel sapphire contacts. In both cases, the enhancement of the excellent tribological performance of the neat IL is due to the more effective lubrication during the running-in period in the presence of graphene, before the formation of stable films of adsorbed IL molecules on the sliding surfaces.

Surface modification of 1-10 layers graphene by ionic liquid molecules prevents agglomeration. For an effective lubrication the graphene sheets must remained dispersed in the base lubricant, in order to prevent abrasion of the sliding surfaces. Long-term sliding tests will be carried out in order to determine the stability of 1-10 layers grapheme, as the contact conditions could give rise to fewer layers grapheme structures.

Acknowledgements

The authors thank the financial support of the Ministerio de Economia y Competitividad (MINECO, Spain; FEDER, EU) (Grant MAT2014-55384-P). "*Este trabajo es resultado de los proyectos de investigación* (19292/PI/14, 19544/GERM/14 and 19877/GERM/14) *financiados por la Fundación Séneca-Agencia de Ciencia y Tecnología de la Región de Murcia en el marco del PCTIRM2011-2014*". N. Saurin is grateful to MINECO (Spain) for a FPI research Grant (BES-2012-056621).

References

[1]. I. Suarez-Martinez, N. Grobert, C.P. Ewels, Carbon 50 (2012) 741-747.
[2]. A.K. Geim, Graphene: status and prospect. Science 324 (2009) 1530-1534.
[3]. W.W. Liu, S.P. Chai, A.R. Mohamed, U. Hashim, J. Ind. Eng. Chem. 20 (2014) 1171-1185.
[4]. D. Berman, A. Erdemir, A.V. Sumant, Mater. Today 17 (2014) 31-42.
[5]. O. Penkov, H.J. Kim, D.E. Kim, Int. J. Precis. Eng. Manufact. 15(2014)577-585.
[6]. X.Q. Fan, Y.Q. Xia, L.P. Wang, W. Li. Tribol. Lett. 55 (2014) 455-464.
[7]. G.Y. Bai, J.Q. Wang, Z.G. Yang, H.G. Wang, Z.F. Wang, S.R. Yang, RSC Adv., 4 (2014) 47096-47105.
[8]. S. Choudhary, H.P. Mungse, O.P. Khatri, J. Mater. Chem. 22 (2012) 21032-21039.
[9]. H.P Mungse, O.P. Khatri, J. Phys. Chem. C 118 (2014) 14394-14402.
[10]. Z. Liu, Nanotechnology, 25 (7) (2014).
[11]. S.S. Kandanur, M.A. Rafiee, F. Yavari, M. Schrameyer, Z.Z. Yu, T.A. Blanchet, N. Koratkar, Carbon 50 (2012) 3178–3183.
[12]. X.J. Shen, X.Q. Pei, Y. Liu, S.Y. Fu, Compos. Part B-Eng. 57 (2014) 120-125.
[13]. J. Sanes, F.J. Carrión, M.D. Bermudez, E-Polymer No. 005 (2007).
[14]. J. Sanes, F.J. Carrión, M.D. Bermúdez, Wear 268 (2010) 1295–1302.
[15]. M.D. Bermúdez, A.E. Jiménez, J. Sanes, F.J. Carrión, Molecules 14 (2009) 2888-2908.
[16]. I. Minami, Molecules 14 (2009) 2262-2269.
[17]. F. Zhou, Y. Liang, W. Liu, Chem. Soc. Rev. 38 (2009) 2590-2599.
[18]. M. Palacio, B.A. Bhushan, Tribol. Lett. 40 (2010) 247-268.
[19]. A.E. Somers, P.C. Howlett, D.R. MacFarlane, M. Forsyth, Lubricants 1(2013) 3–21.
[20]. J. Liu, J. Tang, J.J. Gooding, J. Mater. Chem. 22 (2012) 12435–12452.
[21]. W. Zhao, Z. Zeng, S. Peng, X. Wu, Q. Xue, J. Chen, Tribol. Trans. 56 (2013) 480-487.
[22]. V. Khare, M.Q. Pham, N. Kumari, H.S. Yoon, C.S. Kim, J.I. Park, S.h. Ahn, ACS Appl. Mater. Interfaces 5 (2013) 4063-4075.
[23]. N. Saurín, J. Sanes, M.D. Bermudez, Tribol. Lett. 56 (2014) 133-142.